

Indicator Simulation Accounting for Multiple-Point Statistics

Julián M. Ortiz ¹ and Clayton V. Deutsch ²

Geostatistical simulation aims at reproducing the variability of the real underlying phenomena. When non linear features or large range connectivity are present, the traditional variogram-based simulation approaches do not provide good reproduction of those features. Connectivity of high and low values is often critical for grades in a mineral deposit. Multiple-point statistics can help to characterize these features.

The use of multiple-point statistics in geostatistical simulation was proposed more than ten years ago, based on the use of training images to extract the statistics. This paper proposes the use of multiple-point statistics extracted from actual data.

A method is developed to simulate continuous variables. The indicator kriging probabilities used in sequential indicator simulation are modified by probabilities extracted from multiple-point configurations. The correction is done under the permanence of ratios assumption.

The practical implementation of the method is illustrated with data from a porphyry copper mine.

KEYWORDS: geostatistics, multiple-point statistics inference, sequential indicator simulation, permanence of ratios.

Introduction

Geostatistical realizations permit the calculation of *joint uncertainty*, that is, the uncertainty over arbitrary large volumes. For example, the probability and grades of selective mining units above specified cutoffs can be obtained from a suite of simulated realizations. Estimates can be obtained from multiple realizations under any measure of goodness, not only the minimization of the mean squared estimation error (Deutsch, 2002; Journel, 1989).

Conventional simulation techniques account only for two-point statistics through a covariance (or variogram) model. The use of multiple-point statistics was proposed more than ten years ago (Deutsch, 1992; Guardiano and Srivastava, 1993), however, all developments have been based on the use of training images for extracting the multiple-point statistics. These methods have limited applicability in the mining industry.

After a brief review of the attempts at using multiple-point statistics in simulation, we propose a method to integrate the indicator kriging probability with a multiple-point probability. This probability could be obtained from a training image or extracted from data. We propose the use of production (blasthole) data to infer multiple-point statistics.

¹Department of Civil & Environmental Engineering, 220 Civil / Electrical Engineering Building, University of Alberta, Edmonton, Alberta, CANADA, T6G 2G7. e-mail: jmo1@ualberta.ca

²Department of Civil & Environmental Engineering, 220 Civil / Electrical Engineering Building, University of Alberta, Edmonton, Alberta, CANADA, T6G 2G7. e-mail: cdeutsch@civil.ualberta.ca

Attempts at Multiple-Point Geostatistics

Indicator algorithms allow different characterization of the continuity at different thresholds, which cannot be controlled by Gaussian methods (Journel, 1983). Some novel applications of conventional simulation techniques show improvements over typical applications, by incorporating local directions of anisotropy (Deutsch and Lewis, 1992) or by correcting the variogram range to account for the additional connectivity not captured by the variogram (Deutsch and Gringarten, 2000). Connectivity of extremes can also be controlled by defining a bivariate law in a framework similar to disjunctive kriging (Emery, 2002). These methods do not directly use multiple-point statistics into simulation. Algorithms that only account for two-point statistics cannot reproduce some features that are captured by higher-order statistics.

Object-based methods are used to characterize large curvilinear or connected features first and then conventional two-point statistics could be used to simulate the petrophysical variable inside the different objects (Deutsch and Wang, 1996; Georgsen and Omre, 1993; Haldorsen and MacDonald, 1987). Inference of the parameters to define the orientation and shape of these objects, and conditioning the models to data are two challenges of object-based methods.

The direct use of multiple-point statistics in simulation has been addressed several times. Guardiano and Srivastava introduced the generalization of the indicator algorithm and use of the extended normal equations (Guardiano and Srivastava, 1993; Journel, 1993). The implementation of this technique was improved by Strebelle and Journel, by using a search tree to find the frequencies of the multiple-point events in the training image (Strebelle and Journel, 2000). Deutsch applied simulated annealing for constructing reservoir models with multiple-point statistics (Deutsch, 1992). The difficult setting of the annealing schedule and high computational cost of this technique makes it unappealing to practitioners. Another interesting implementation of simulated annealing was proposed by Srivastava to simulate using change of support statistics, indirectly accounting for multiple-point statistics (Srivastava, 1994). Another iterative technique was proposed by Caers that is based on the use of neural networks to model the conditional distribution function in a non-linear fashion (Caers, 1998).

Most previous proposals were aimed at petroleum applications. All implementations assume that multiple-point statistics are available. In petroleum applications, few local data are available, hence training images are considered for inferring multiple-point statistics. One concern is the reproduction of features that belong to the training image, but not to the underlying process that is being simulated. We may want to reproduce the general appearance of the training image but not all its details. Caers proposed to split the training data into a training set and a validation set. Then, the validation set can be used to detect when the training of the neural network is overfitting the training set (Caers, 1998). However, the question of which features should be extracted from the training image is difficult and unavoidably subjective. Furthermore, transferring statistics from the training image to the realization is a problem. The univariate and bivariate statistics of the training image may not be exactly the same as those of the study area.

We propose a method to integrate multiple-point statistics into geostatistical simulation. The method is general and could be applied in petroleum or mining. We demonstrate the

implementation of the proposed method with a mining case study, where the multiple-point statistics are extracted from production data, rather than a training image. Data come from deemed representative mined out areas. The more statistics we can reliably infer from the data and pass into the simulated realizations, the better the performance of the numerical models.

Statistical Inference of Multiple-Point Statistics

The probabilities of multiple-point events can be estimated by their relative frequencies found in a dataset. Of course, inference will only be possible if multiple replications of an event are available to calculate its frequency. In practice most of the samples are taken at drillholes as almost linear strings. The frequencies of low-order statistics (three to five point configurations), such as the indicator values for strings of multiple composites in the vertical direction may be calculated. It would be difficult to use drillhole data to infer curvilinear features. Closely spaced blasthole data may be useful.

Stationarity must be assumed. The decision must be made to pool data together for inference. The simulated realizations may not perform well if the data are not representative of the domain under study. Of course, the resulting simulated models will also be unreliable if there are not enough data to infer the required statistics.

The application of conventional kriging-based geostatistical simulation requires consistent or positive-definite statistics. We propose an updating approach that removes the need for positive-definiteness of the models. Any inconsistency will be reflected as order relations in the final conditional distributions, as it occurs in indicator kriging-based methods.

Updating the Indicator Kriging Probability with Multiple-Point Statistics

We are interested in calculating the probability of a variable Z not to exceed a threshold z_k at location \mathbf{u} , which we will call event \mathbf{A} . We have a number of events R that inform this location, noted as $\mathbf{B}_1, \dots, \mathbf{B}_R$, to calculate the conditional probability of \mathbf{A} at \mathbf{u} . These R events may correspond to any arrangement of any number of data at any volume support. They can be disjoint or have elements in common. They can be considered as sets of elements, such as the samples used in kriging to estimate the value at an unsampled location, or they can be considered as a joint event, such as a multiple-point event, that is, a configuration of multiple samples.

Consider the case where information from several different sources is used to estimate the conditional probability of event \mathbf{A} . Bayes' law gives a formalism to calculate this conditional probability. These different sources of information can be integrated to estimate the posterior conditional probability of \mathbf{A} :

$$P(\mathbf{A}|\mathbf{B}_1, \dots, \mathbf{B}_R) = \frac{P(\mathbf{A}, \mathbf{B}_1, \dots, \mathbf{B}_R)}{P(\mathbf{B}_1, \dots, \mathbf{B}_R)} \quad (1)$$

This expression requires the knowledge of the joint distribution of the events $\mathbf{B}_1, \dots, \mathbf{B}_R$ with event \mathbf{A} , that is, $P(\mathbf{A}, \mathbf{B}_1, \dots, \mathbf{B}_R)$, and the joint distribution of the events informing \mathbf{A} , $P(\mathbf{B}_1, \dots, \mathbf{B}_R)$. These multivariate distributions are difficult to infer.

Recursive application of Bayes' law permits **Equation 1** to be rewritten as:

$$P(\mathbf{A}|\mathbf{B}_1, \dots, \mathbf{B}_R) = \frac{P(\mathbf{B}_R|\mathbf{A}, \mathbf{B}_1, \dots, \mathbf{B}_{R-1}) \cdot P(\mathbf{B}_{R-1}|\mathbf{A}, \mathbf{B}_1, \dots, \mathbf{B}_{R-2}) \cdots P(\mathbf{B}_1|\mathbf{A}) \cdot P(\mathbf{A})}{P(\mathbf{B}_1, \dots, \mathbf{B}_R)} \quad (2)$$

This expression can be simplified under assumptions of conditional independence, which will allow the calculation of the numerator. If two expressions with the same denominator are considered, the expression in the denominator does not need to be known, since it can be removed by taking a ratio between them.

Permanence of Ratios Assumption

The assumption of permanence of ratios is a way around the problem of knowing the joint probabilities of $\mathbf{B}_1, \dots, \mathbf{B}_R$ and $\mathbf{A}, \mathbf{B}_1, \dots, \mathbf{B}_R$ (Journel, 1993; Journel, 2002). Conditional independence between the events $\mathbf{B}_i, i = 1, \dots, R$ given \mathbf{A} is assumed. This corresponds to the same assumption of the Naive-Bayes model in statistical classification and it is usually depicted as a Bayesian network (**Figure 1**) (Frank and others, 2000; Friedman, 1997; Friedman and others, 1997; Ramoni and Sebastiani, 2001).

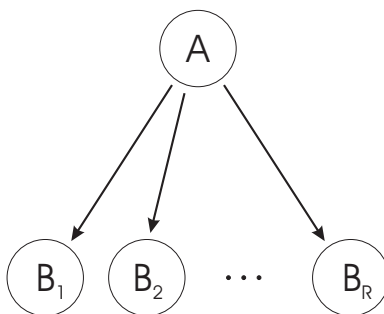


Figure 1: Bayesian network representing the Naive Bayes classifier with attributes $\mathbf{B}_1, \mathbf{B}_2, \dots, \mathbf{B}_R$. The conditional independence assumption is shown as no connectors between the attributes.

This assumption basically states that the incremental information provided by one event \mathbf{B}_i before and after knowing the others is constant. It originates from the assumption of conditional independence between the sources of information, given the event \mathbf{A} :

$$\begin{aligned} P(\mathbf{B}_R|\mathbf{A}, \mathbf{B}_1, \dots, \mathbf{B}_{R-1}) &= P(\mathbf{B}_R|\mathbf{A}) \\ P(\mathbf{B}_{R-1}|\mathbf{A}, \mathbf{B}_1, \dots, \mathbf{B}_{R-2}) &= P(\mathbf{B}_{R-1}|\mathbf{A}) \\ &\vdots \\ P(\mathbf{B}_2|\mathbf{A}, \mathbf{B}_1) &= P(\mathbf{B}_2|\mathbf{A}) \end{aligned}$$

The conditional probability in **Equation 2** can now be written:

$$P(\mathbf{A}|\mathbf{B}_1, \dots, \mathbf{B}_R) = \frac{P(\mathbf{B}_R|\mathbf{A}) \cdot P(\mathbf{B}_{R-1}|\mathbf{A}) \cdots P(\mathbf{B}_1|\mathbf{A}) \cdot P(\mathbf{A})}{P(\mathbf{B}_1, \dots, \mathbf{B}_R)} \quad (3)$$

We can also write the expression for the conditional probability of \mathbf{A} not occurring (the complement of \mathbf{A} , which we will denote $\bar{\mathbf{A}}$). Under a similar assumption of conditional independence, we have:

$$P(\bar{\mathbf{A}}|\mathbf{B}_1, \dots, \mathbf{B}_R) = \frac{P(\mathbf{B}_R|\bar{\mathbf{A}}) \cdot P(\mathbf{B}_{R-1}|\bar{\mathbf{A}}) \cdots P(\mathbf{B}_1|\bar{\mathbf{A}}) \cdot P(\bar{\mathbf{A}})}{P(\mathbf{B}_1, \dots, \mathbf{B}_R)} \quad (4)$$

And taking the ratio between **Equations 4** and **3**, we get rid of the joint probability of the conditioning events $\mathbf{B}_1, \dots, \mathbf{B}_R$:

$$\frac{P(\bar{\mathbf{A}}|\mathbf{B}_1, \dots, \mathbf{B}_R)}{P(\mathbf{A}|\mathbf{B}_1, \dots, \mathbf{B}_R)} = \frac{P(\mathbf{B}_R|\bar{\mathbf{A}}) \cdot P(\mathbf{B}_{R-1}|\bar{\mathbf{A}}) \cdots P(\mathbf{B}_1|\bar{\mathbf{A}}) \cdot P(\bar{\mathbf{A}})}{P(\mathbf{B}_R|\mathbf{A}) \cdot P(\mathbf{B}_{R-1}|\mathbf{A}) \cdots P(\mathbf{B}_1|\mathbf{A}) \cdot P(\mathbf{A})} \quad (5)$$

Equation 5 can be rewritten as:

$$\frac{P(\bar{\mathbf{A}}|\mathbf{B}_1, \dots, \mathbf{B}_R)}{P(\mathbf{A}|\mathbf{B}_1, \dots, \mathbf{B}_R)} = \frac{\frac{P(\bar{\mathbf{A}}|\mathbf{B}_R) \cdot P(\mathbf{B}_R)}{P(\bar{\mathbf{A}})} \cdot \frac{P(\bar{\mathbf{A}}|\mathbf{B}_{R-1}) \cdot P(\mathbf{B}_{R-1})}{P(\bar{\mathbf{A}})} \cdots \frac{P(\bar{\mathbf{A}}|\mathbf{B}_1) \cdot P(\mathbf{B}_1)}{P(\bar{\mathbf{A}})} \cdot P(\bar{\mathbf{A}})}{\frac{P(\mathbf{A}|\mathbf{B}_R) \cdot P(\mathbf{B}_R)}{P(\mathbf{A})} \cdot \frac{P(\mathbf{A}|\mathbf{B}_{R-1}) \cdot P(\mathbf{B}_{R-1})}{P(\mathbf{A})} \cdots \frac{P(\mathbf{A}|\mathbf{B}_1) \cdot P(\mathbf{B}_1)}{P(\mathbf{A})} \cdot P(\mathbf{A})} \quad (6)$$

since,

$$P(\mathbf{B}_i|\mathbf{A}) = \frac{P(\mathbf{A}, \mathbf{B}_i)}{P(\mathbf{A})} = \frac{P(\mathbf{A}|\mathbf{B}_i) \cdot P(\mathbf{B}_i)}{P(\mathbf{A})}$$

We can simplify **Equation 6** to write the general expression for the permanence of ratios assumption to integrate information from several sources:

$$P(\mathbf{A}|\mathbf{B}_1, \dots, \mathbf{B}_R) = \frac{\left(\frac{P(\bar{\mathbf{A}})}{P(\mathbf{A})}\right)^{R-1}}{\left(\frac{P(\bar{\mathbf{A}})}{P(\mathbf{A})}\right)^{R-1} + \prod_{i=1}^R \frac{P(\bar{\mathbf{A}}|\mathbf{B}_i)}{P(\mathbf{A}|\mathbf{B}_i)}} \quad (7)$$

This expression does not require a prior knowledge of the relationships between the events $\mathbf{B}_i, i = 1, \dots, R$, that is, all conditional relationships are built based on the assumption that the incremental information provided by the event \mathbf{B}_i regarding the event \mathbf{A} is constant regardless of the other conditioning events. The permanence of ratios assumption greatly simplifies the calculation of the conditional probability.

Methodology

Sequential indicator simulation works by discretizing the conditional distributions by a set of probabilities calculated for some threshold values. The probabilities assigned to each threshold are calculated by simple indicator kriging the data and previously simulated indicator values. The estimated indicator value is the conditional probability at that threshold, that is, it corresponds to the probability for that unsampled location to have a value less than or equal to the threshold value. Once these probabilities have been estimated for the

set of thresholds, a simulated value is drawn by considering some interpolation between the thresholds and extrapolation beyond the lowest and highest thresholds. Simple indicator kriging does not ensure that the estimated probabilities for a given node will be a non-decreasing function between 0 and 1, which is a necessary condition for a cumulative conditional distribution. Order relation deviations are corrected to ensure that a valid cumulative distribution is built at every location prior to simulating the value. Sequential indicator simulation allows obtaining the conditional probability at an unsampled location (event \mathbf{A}), given the set of n_{B_1} single-point events provided by the indicator coded sample data and previously simulated nodes. Together, these n_{B_1} events define the event \mathbf{B}_1 . Indicator kriging provides the conditional probability $P(\mathbf{A}|\mathbf{B}_1)$, which only accounts for two-point statistics: the indicator covariances between indicator coded samples and previously simulated nodes and between them and the location of interest.

The multiple-point set of nearby or adjacent samples is denoted \mathbf{B}_2 . The conditional probabilities of type $P(\mathbf{A}|\mathbf{B}_2)$ can be calibrated with multiple-point statistics obtained from configurations of the conditioning information (indicator coded samples and previously simulated nodes). These multiple-point statistics are estimated from the frequencies of a fixed set of spatial configurations, extracted from production information from a set of mined out benches. If informed, any arrangement of the four adjacent nodes to the one being simulated can be considered to extract a probability of the indicator value at the location of interest, given the indicator codes at the same threshold for the informed adjacent nodes. The multiple-point event, formed in this case by $n_{B-2} = 2, 3, \text{ or } 4$ nodes, allows the inference of $P(\mathbf{A}|\mathbf{B}_2)$.

The integration of both sources of information is made under the assumption of permanence of ratios, which allows the calculation of $P(\mathbf{A}|\mathbf{B}_1, \mathbf{B}_2)$ without requiring the joint distribution of \mathbf{B}_1 and \mathbf{B}_2 .

The general framework presented in the previous section is used to integrate information from two sources to a dataset from an operating mine. The two sources of information are: (1) exploration sample data and (2) production data. The methodology for integrating these sources of information can be summarized as:

1. Estimate the indicator values for several thresholds by simple indicator kriging with the exploration sample data.
2. Estimate the conditional probability given a set of multiple-point configurations from blasthole data. These conditional probabilities are inferred from the frequency of blasthole samples being below a threshold, given the values of surrounding blastholes.
3. Integrate the two conditional probabilities from indicator kriging and from the multiple-point configuration by permanence of ratios.

A **GSLIB**-type program to calculate the conditional probabilities given multiple-point information was prepared. The integration of the two sources of information under the permanence of ratios assumption was performed with a modified version of the program **SISIM** in **GSLIB** (Deutsch and Journel, 1997).

It is worth noticing that the assumption of permanence of ratios does not distinguish between the two cases presented schematically in **Figure 2**. The two sources of information

are deemed independent of each other, when they are used to estimate \mathbf{A} . Screening and redundancy of the information from several sources is not explicit when assuming conditional independence.

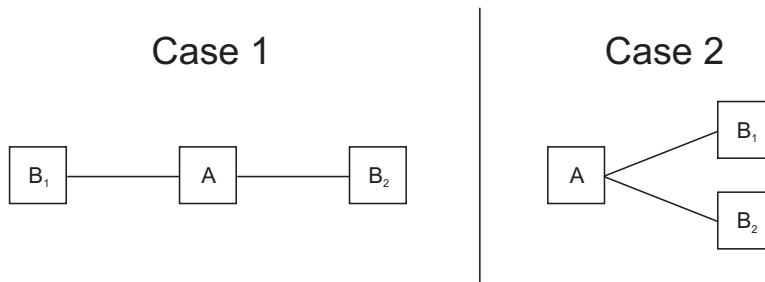


Figure 2: The assumption of conditional independence of the sources of information given the event of interest is highlighted in this schematic example. The assumption cannot distinguish between Case 1 and Case 2. The redundancy between the events and possible screening is not accounted for: data events \mathbf{B}_1 and \mathbf{B}_2 are more redundant in Case 2.

Case Study: Porphyry Copper Deposit

The objective of this case study is to show the implementation of the methodology presented and discuss some of the details of integrating information from multiple sources. Conventional sequential indicator simulation and the proposed method accounting for multiple-point statistics are considered.

In this application, the event \mathbf{A} is the probability of a given uninformed node at location \mathbf{u} to be below the current threshold z_k , for K thresholds. Two sources of information are available. We call \mathbf{B}_1 the set of single points found within a search neighborhood that are used to estimate the probability at \mathbf{u} (event \mathbf{A}), by simple indicator kriging. They correspond to individual drillhole composites. This means that $P(\mathbf{A}|\mathbf{B}_1)$ is the simple indicator kriging estimate at \mathbf{u} . A second source of information comes from the blasthole dataset. We call \mathbf{B}_2 the event of having any multiple-point configuration depicted in **Figure 3** around \mathbf{u} . The conditional probability of the event \mathbf{A} at location \mathbf{u} is estimated based on the availability of sample data or previously simulated nodes at the four nodes adjacent to \mathbf{u} . This multiple-point probability corresponds to $P(\mathbf{A}|\mathbf{B}_2)$. The proposed indicator simulation method under the assumption of permanence of ratios provides an estimate for the conditional probability at \mathbf{u} based on both sources of information:

$$P(\mathbf{A}|\mathbf{B}_1, \mathbf{B}_2) = \frac{\frac{P(\bar{\mathbf{A}})}{P(\mathbf{A})}}{\frac{P(\bar{\mathbf{A}})}{P(\mathbf{A})} + \frac{P(\bar{\mathbf{A}}|\mathbf{B}_1)}{P(\mathbf{A}|\mathbf{B}_1)} \cdot \frac{P(\bar{\mathbf{A}}|\mathbf{B}_2)}{P(\mathbf{A}|\mathbf{B}_2)}} \quad (8)$$

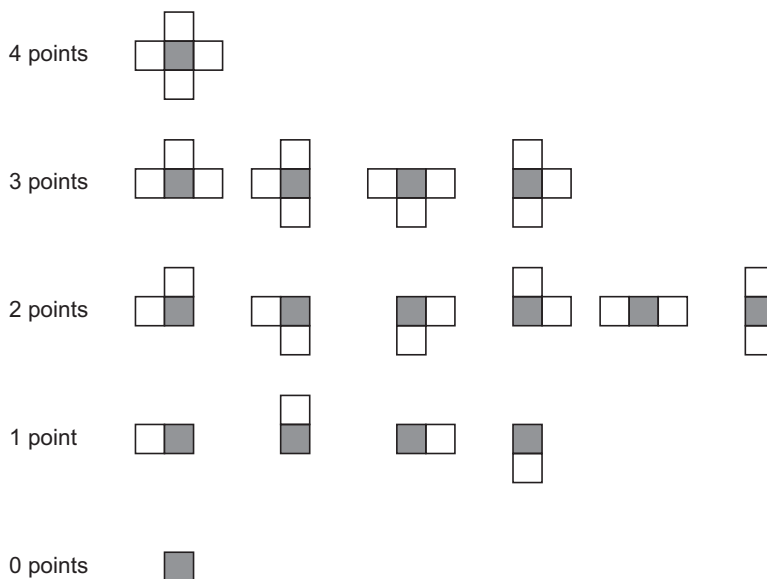


Figure 3: Multiple-point patterns with adjacent grid nodes. The gray node is the one being estimated. The patterns correspond to the four adjacent nodes to the node of interest. The probabilities are extracted from the blasthole dataset even when some of the nodes are not informed, generating the three-, two-, one-, and zero-point patterns.

Data

Two datasets are available for this study. The data correspond to copper grades from drillhole and blasthole samples for several benches of a porphyry copper deposit.

The drillhole database has 12m composites, that correspond to the bench height. Several rock types are available, but only one homogeneous geological population is presented here. A plan view of the drillhole data for one bench is presented in **Figure 4**. The average spacing between drillholes is around 50 m.

Blastholes for several benches are available. Blastholes are drilled at the bench height. A view of the blasthole information for one bench is presented in **Figure 5**. The samples are regularly spaced on a 10 by 10 m. grid. Blastholes are more irregular in the perimeter where damage control on the walls requires a closer spacing. Although the blastholes appear like an exhaustive sampling, they represent less than $1/1000^{th}$ of the rock mass and provide little information on the heterogeneity at less than 10m spacing.

The blasthole information from the two lower benches is kept aside for the final comparison of performance of the methods.

Declustering is required to obtain a representative reference distribution for simulation. A cell declustering procedure is applied to find the cell size that minimizes the mean. Given the spacing of the data an anisotropic cell is used with a horizontal to vertical size ratio of 4 to 1, since the vertical spacing of the samples is 12 m and the drillhole spacing is approximately 50 m. A cell size of $120 \times 120 \times 30 m^3$ was chosen based on the summary declustered mean versus cell size plot. The declustering weights are used to correct the

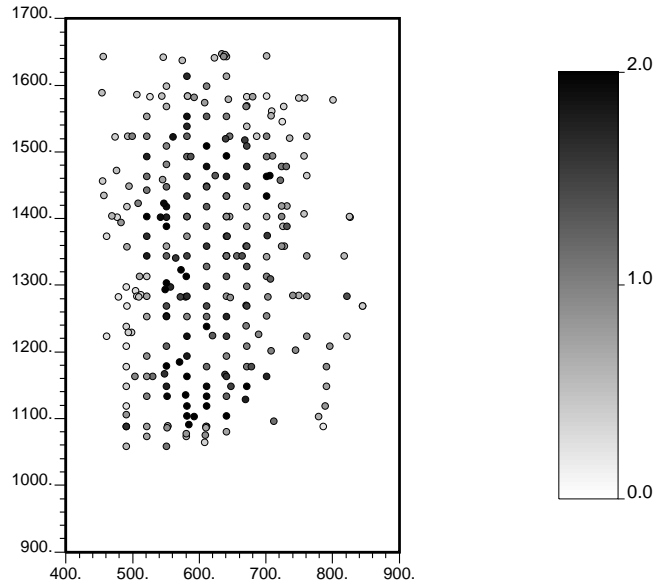


Figure 4: Plan view showing the drillhole information for a particular bench.

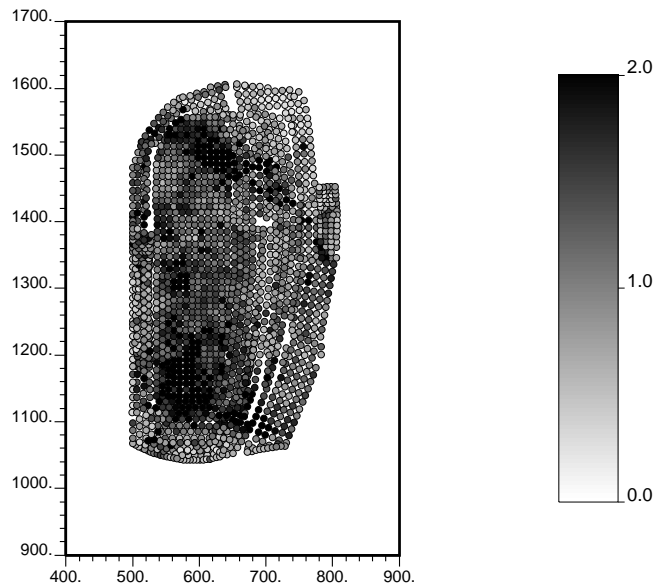


Figure 5: Plan view showing the blasthole information for a particular bench.

cumulative distribution function value below each threshold. The procedure generates a distribution with a mean of 1.068 %Cu. The original value was 1.157 %Cu. The standard deviation remained unchanged at 0.548 %Cu. The mean of the blasthole data used to infer the variograms and multiple-point statistics is 1.249 %Cu with a standard deviation of 0.620 %Cu.

Threshold number	1	2	3	4	5	6	7	8	9	10
Threshold value	0.58	0.73	0.84	0.95	1.08	1.22	1.36	1.56	1.91	2.18
Clustered quantile	0.10	0.20	0.30	0.40	0.50	0.60	0.70	0.80	0.90	0.95
Declustered quantile	0.15	0.28	0.38	0.47	0.57	0.68	0.76	0.85	0.93	0.97

Table 1: Threshold definition for indicator variogram calculation and simulation.

Comparison of Datasets

The two datasets have been validated by the mine staff and are considered unbiased. Statistics from the drillhole and blasthole datasets were compared. Paired samples from both databases correlate quite well. The correlation between the two datasets can be reasonably extrapolated to 1.0 at $\mathbf{h} = 0$, since a correlation coefficient $\rho = 0.64$ for pairs up to 10m apart is obtained and the relative nugget effect is 0.30. Trends show the same behavior in the three principal directions for both datasets. Trends are not pronounced. Enough conditioning information is available to control any local variation of the mean and variance.

Variogram Modelling

Ten thresholds are used to obtain an adequate discretization of the conditional distributions. The selection of these 10 values calls for several considerations: the full distribution should be adequately sampled by these values, that is, selecting values that are regularly spaced (in terms of probabilities) is convenient because interpolation between thresholds is simplified; the adequate characterization of high grades is required, hence additional thresholds are located in the high tail of the distribution, however, variogram inference becomes more difficult as the threshold is more extreme. The 10 threshold values correspond to the nine deciles in the clustered distribution, and an additional threshold at the quantile 0.95. This last value will help characterizing the high values, minimizing extrapolation problems due to the skewness of the distribution. The proportions below the thresholds considering the declustering weights are used within the indicator simulation.

Table 1 shows the threshold values, proportions that fall below that threshold in the clustered distribution, and the proportions corrected to account for the clusters.

The main directions of anisotropy were found at N30°W, N60°E, and vertical. This is consistent with the geology of the region, and with previous studies over this area.

Variogram modelling considers that variogram models for adjacent thresholds must be consistent and will likely vary smoothly.

Table 2 shows the parameters for the models fitted to the experimental variograms. Three structures are used to model the variogram: two spherical and one exponential. The nugget effect is smaller for thresholds far from the median, opposite to what is obtained using a multi-Gaussian method. Ranges tend to decrease as the cutoff increases, which is consistent with the multi-Gaussian model.

Cutoff	Nugget Effect	Spherical						Spherical						Exponential					
		Sill		Range		Vert.		Sill		Range		Vert.		Sill		Range		Vert.	
		N30°W	N60°E	N30°W	N60°E	Vert.	N30°W	N60°E	Vert.	N30°W	N60°E	Vert.	N30°W	N60°E	Vert.	N30°W	N60°E	Vert.	
0.58	0.30	0.25	25.0	40.0	30.0	0.27	480.0	380.0	45.0	0.18	∞	280.0	∞	∞	∞	280.0	∞	∞	
0.73	0.30	0.25	25.0	40.0	20.0	0.27	200.0	220.0	30.0	0.18	∞	200.0	∞	∞	∞	200.0	∞	∞	
0.84	0.30	0.25	25.0	40.0	25.0	0.25	200.0	140.0	35.0	0.20	320.0	180.0	∞	∞	∞	180.0	∞	∞	
0.95	0.30	0.25	40.0	70.0	30.0	0.25	160.0	100.0	40.0	0.20	180.0	120.0	∞	∞	∞	120.0	∞	∞	
1.08	0.35	0.20	40.0	65.0	40.0	0.25	130.0	85.0	130.0	0.20	130.0	80.0	130.0	130.0	130.0	80.0	130.0	130.0	
1.22	0.35	0.20	40.0	35.0	50.0	0.25	90.0	85.0	130.0	0.20	110.0	80.0	130.0	130.0	130.0	80.0	130.0	130.0	
1.36	0.30	0.25	35.0	30.0	60.0	0.25	80.0	65.0	130.0	0.20	90.0	75.0	130.0	130.0	130.0	75.0	130.0	130.0	
1.56	0.30	0.30	35.0	30.0	60.0	0.20	70.0	65.0	140.0	0.20	60.0	55.0	140.0	140.0	140.0	55.0	140.0	140.0	
1.91	0.25	0.40	25.0	20.0	50.0	0.15	60.0	55.0	150.0	0.20	60.0	55.0	150.0	150.0	150.0	55.0	150.0	150.0	
2.18	0.20	0.40	20.0	20.0	28.0	0.15	35.0	35.0	∞	0.25	40.0	40.0	∞	∞	∞	40.0	∞	∞	

Table 2: Standardized indicator variogram model parameters.

Direction	Number of nodes	Grid spacing
Easting	50	10.0
Northing	80	10.0

Table 3: Grid definition for multiple-point inference and simulation.

Multiple-Point Statistics Inference

Blasthole data are used to infer multiple-point statistics. The scattered blasthole locations are associated with the closest point on a regular 10m by 10m grid. The frequencies of multiple-point configurations for all the patterns shown in **Figure 3** are inferred. Again, the two benches used for validation are not considered during the inference of multiple-point statistics. Inference is made by simply counting how many times the central node of the multiple-point configuration is below the threshold, given the indicator values of the four adjacent nodes for that same threshold, if informed. This count is divided by the total number of multiple-point events with the same configuration to approximate the frequency of this event.

Figure 6 shows the indicator maps from the blasthole dataset for one bench considering a regular two-dimensional grid defined by the parameters in **Table 3**.

Simulation must be done at the same resolution as the multiple-point information.

Sequential Indicator Simulation

One hundred realizations obtained by sequential indicator simulation (SIS) are generated (Deutsch and Journel, 1997). Thresholds and corrected proportions presented in **Table 1** are used. The conditioning data corresponds to the drillhole samples. Interpolation between thresholds is done linearly, while for the tails, the shape of the global declustered distribution is re-scaled for extrapolation, considering a minimum copper grade of 0.0 % and a maximum of 7.5 %. The grid specification is as defined in **Table 3**. Two benches are simulated. These are the same ones where blasthole information is held for validation. The search parameters are presented in **Table 4**.

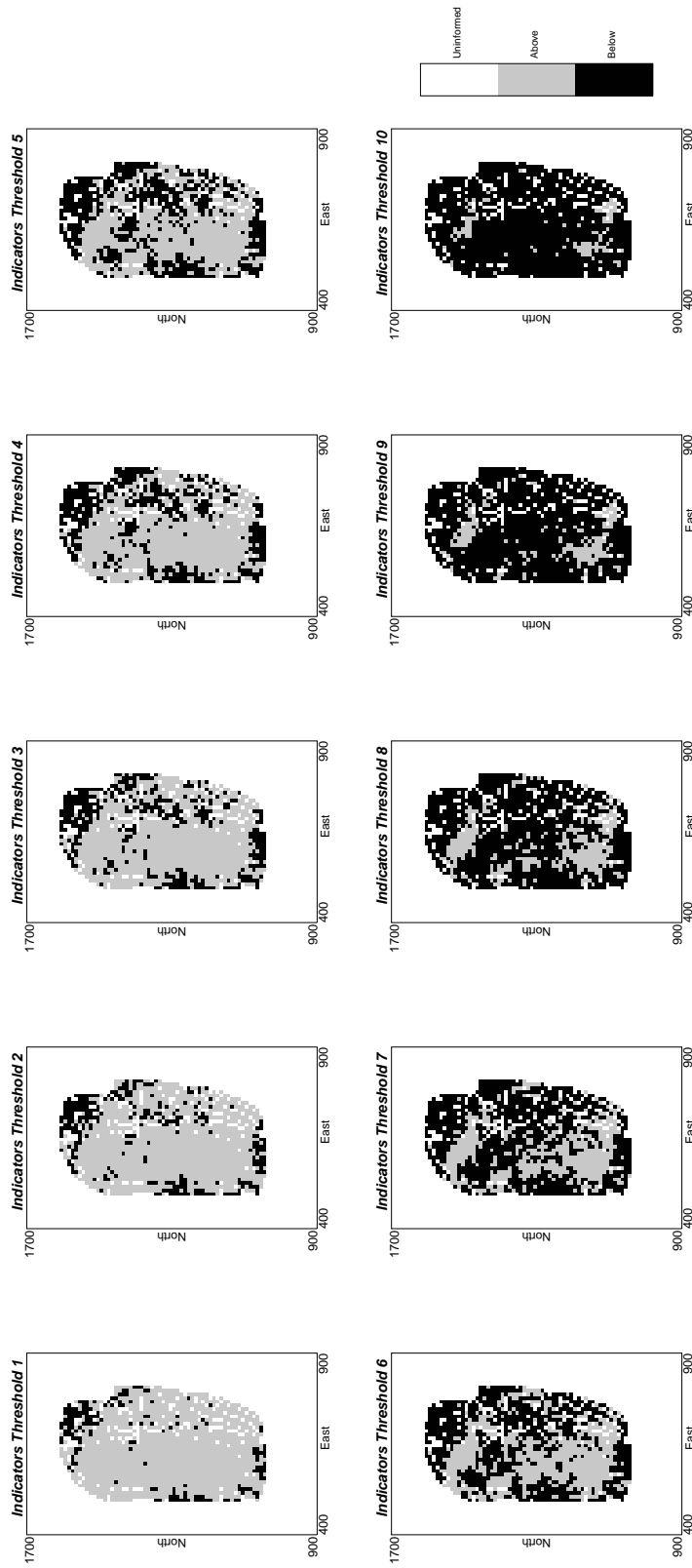


Figure 6: Indicator values of the scattered blasthole data for a particular bench approximated by a regular grid.

Max. data and prev. sim. nodes for kriging	24
Multiple-grid search levels	3
Maximum search radius horiz.	300 m
Maximum search radius vertical	150 m

Table 4: Simulation parameters.

Maps of the two benches for the first two realizations obtained by sequential indicator simulation are presented in **Figure 7**.

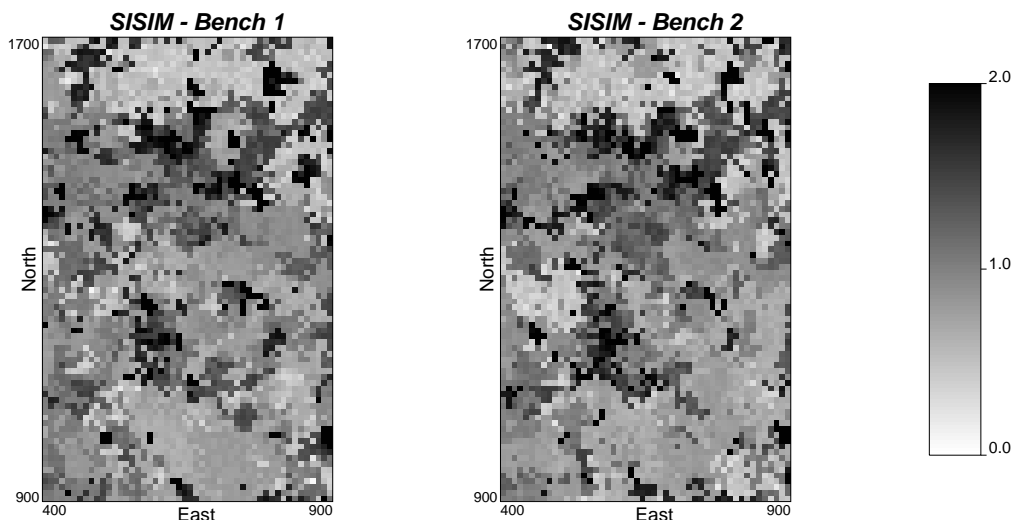


Figure 7: Maps of the two simulated benches for the first two realizations by SIS.

Validation of Results

Realization are checked for data, histogram and indicator variogram reproduction. The mean and the variance of each realization is calculated and plotted on histograms. The reference values are shown as black dots underneath the histograms (**Figure 8**). This graph shows the good reproduction of the histogram.

Order relation deviations occurred in around 52 % of the points simulated with an average magnitude of less than 1.5 %. The maximum correction due to order relation was 20 %. These corrections are within the range that is commonly seen in practice (Deutsch and Journel, 1997). Hence, they are deemed acceptable and should not affect considerably the performance of the numerical models generated.

Sequential Indicator Simulation Accounting for Multiple-Point Statistics

The parameters used to update the indicator kriging probabilities with multiple-point statistics under the assumption of permanence of ratios are the same as before (**Table 4**). Multiple-point statistics are inferred from the two benches above the ones being simulated.

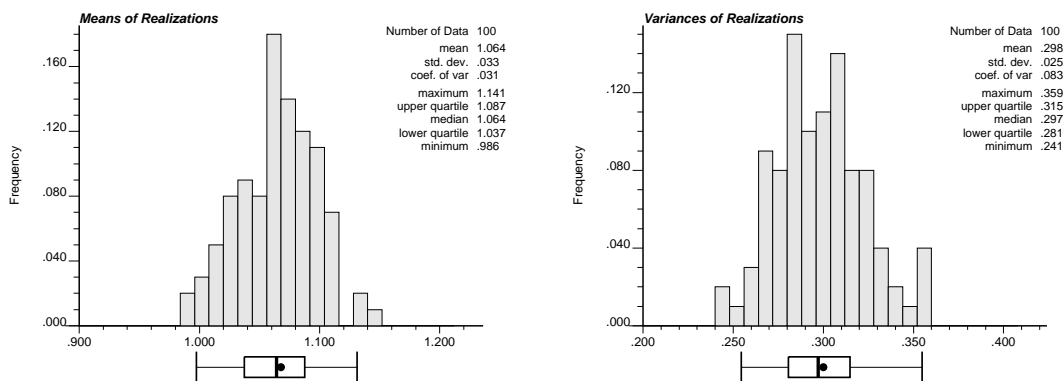


Figure 8: Histograms of the means and variances of the realizations by SIS. The dots below the histogram represent the corresponding reference values.

Validation of Results

The discrepancy between the mean of the drillhole data (1.068 %Cu) and the mean of blastholes used to infer the multiple-point statistics (1.249 %Cu) is corrected by using $P(\mathbf{A})$ obtained from the blasthole grade distribution in **Equation 8**, that is, the proportions for every threshold are calculated from the blasthole dataset. The corrected estimator is unbiased and, as expected, the new implementation results in a much better reproduction of the statistics. The tradeoff is an inflation of the variance of the realizations (**Figure 9**), due to the larger variance of the blasthole data.

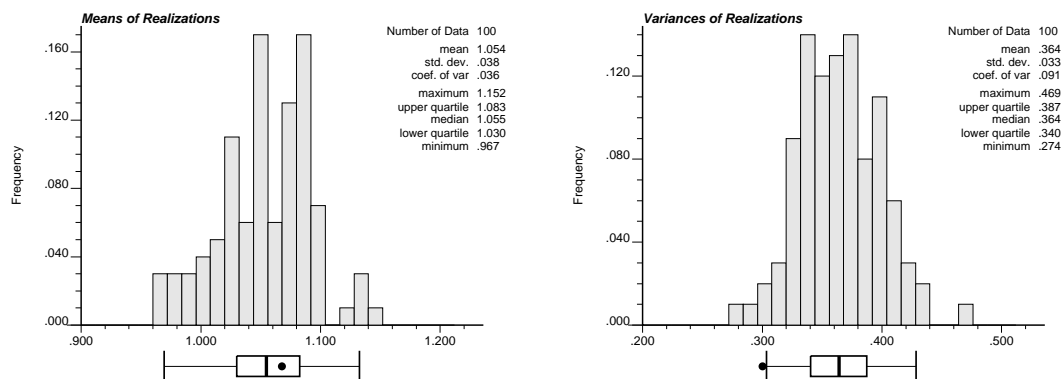


Figure 9: Histograms of the means and variances of the realizations under the assumption of permanence of ratios. The dots below the histogram represent the corresponding reference values.

Maps of the first two realizations are shown in **Figure 10**. Comparing these maps with the ones obtained by SIS (**Figure 7**), the higher connectivity of highs and lows can be appreciated.

As before, the drillhole samples are assigned to the nodes in the grid. The same proce-

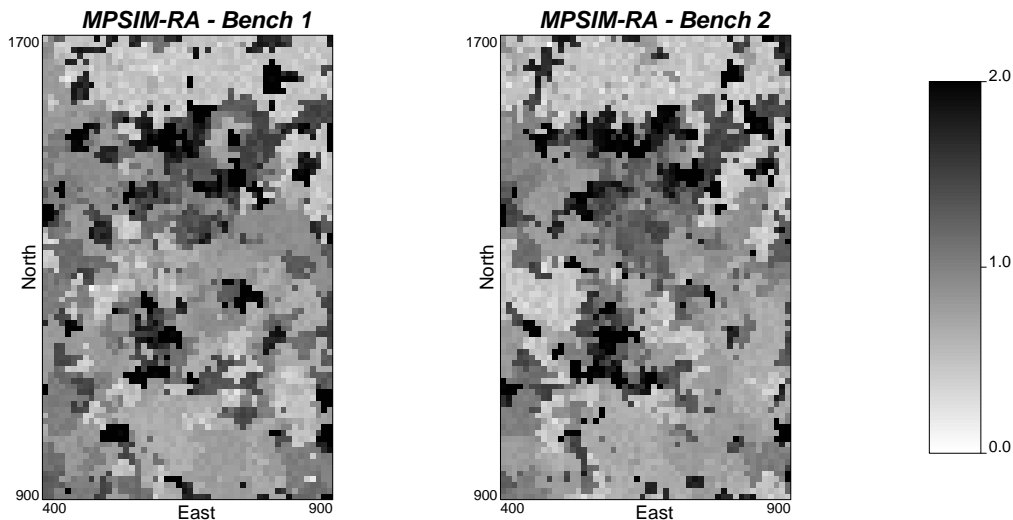


Figure 10: Maps of the two simulated benches for the first two realizations accounting for multiple-point statistics.

ture than in SIS is used and around 90 % of the samples are reproduced, with the other 10 % not assigned to a node because a closer sample was available.

The impact of adding multiple-point information to the models is reflected in the reproduction of the indicator variograms. A slightly larger range is seen in most cases, which is consistent with results obtained by other researchers (Deutsch and Gringarten, 2000).

Order relation deviations are slightly higher than in SIS. Corrections are on average smaller than 2.5 % (compare with .5 % for SIS), with maximums reaching up to 40 % (compare with 20 % for SIS).

Comparison of Results

The average correlation of the simulated nodes with the validation data could be considered: $\rho = 0.30$ for SISIM and $\rho = 0.35$ when multiple-point statistics are used; a significant improvement. The quantity of metal above a cutoff grade of 1.0 %Cu can also be compared to the blastholes kept back: 5.89 % less for SISIM and 2.89 % less when multiple-point statistics are used; a significant improvement. Comparisons are notoriously difficult because it is difficult to arrive at general results. Moreover, the performance of the competing techniques can be very sensitive to many interdependent implementation decisions.

As a final note, we must emphasize that the multiple-point statistics are not honored by the proposed method. However, some of the higher-order features are introduced into the generated models, by locally modifying the probabilities obtained by indicator kriging. The generated models still look like realizations from an indicator method.

Conclusions

Incorporating multiple-point statistics in a Bayesian framework and under the assumption of permanence of ratios between the sources of information can be performed by the proposed indicator technique.

The theoretical framework has been presented for a general case, and the case study showed the implementation details, advantages, and some of the problems that can be encountered in practice.

Inconsistency between the different sources of information is reflected in the final models. This problem was overcome by adjusting the “global” probabilities in the expression to integrate two sources of information. The corrected method gave an unbiased estimate of the conditional probability.

The problem of the resolution (grid spacing) of the multiple-point data and final numerical model was not addressed and remains as a research area in multiple-point geostatistics.

The method could be applied to integrate multiple-point information from more than one source. A straightforward application could be to use the frequencies of multiple-point configurations for three or more adjacent samples in the drillholes in addition to the two-dimensional configurations used in this case study, extracted from blasthole data. This would integrate multiple-point information in three-dimensions to the conventional sequential indicator simulation method.

Comparison of the performance of the models is difficult and deserves further investigation. Historical mill data could be used to evaluate the impact of adding multiple-point information to the models.

References

- Caers, J., 1998, Stochastic simulation with neural networks. In *Report 11, Stanford Center for Reservoir Forecasting*, Stanford, CA, May.
- Deutsch, C. V., 1992, *Annealing Techniques Applied to Reservoir Modeling and the Integration of Geological and Engineering (Well Test) Data*. PhD thesis, Stanford University, Stanford, CA.
- Deutsch, C. V., 2002, *Geostatistical Reservoir Modeling*. Oxford University Press, New York.
- Deutsch, C. V., and Gringarten, E., 2000, Accounting for multiple-point continuity in geostatistics modeling. In *6th International Geostatistical Congress*, Cape Town, South Africa, April. Geostatistical Association of Southern Africa.
- Deutsch, C., and Journel, A., 1998, *GSLIB: Geostatistical software library and users guide*: Oxford University Press, New York, 2nd Edition, 369 p.
- Deutsch, C. V., and Lewis, R. W., 1992, Advances in the practical implementation of indicator geostatistics. In *Proceedings of the 23rd International APCOM Symposium*, pages 133–148, Tucson, AZ, April. Society of Mining Engineers.

- Deutsch, C. V., and Wang, L., 1996, Hierarchical object-based stochastic modeling of fluvial reservoirs. *Mathematical Geology*, 28(7):857–880.
- Emery, X., 2002, Conditional simulation of non-Gaussian random functions. *Mathematical Geology*, 34(1):79–100.
- Frank, E., Trigg, L., Holmes, G., and Witten, I. H., 2000, Technical note: Naive Bayes for regression. *Machine Learning*, 41:5–25.
- Friedman, J. H., 1997, On bias, variance, 0/1-loss, and the curse-of-dimensionality. *Data Mining and Knowledge Discovery*, 1:55–77.
- Friedman, N., Geiger, D., and Goldszmidt, M., 1997, Bayesian network classifiers. *Machine Learning*, 29:131–163.
- Georgsen, F., and Omre, H., 1993, Combining fibre processes and Gaussian random functions for modelling fluvial reservoirs. In A. Soares, editor, *Geostatistics Tróia '92*, volume 1, pages 425–440. Kluwer.
- Guardiano, F., and Srivastava, M., 1993, Multivariate geostatistics: Beyond bivariate moments. In A. Soares, editor, *Geostatistics Tróia '92*, volume 1, pages 133–144. Kluwer.
- Haldorsen, H., and MacDonald, C., 1987, Stochastic modeling of underground reservoir facies. In *62nd Annual Technical Conference and Exhibition Formation Evaluation and Reservoir Geology*, pages 575–589, Dallas, TX, September. Society of Petroleum Engineers. SPE paper # 16751.
- Journel, A., 1993, Geostatistics: Roadblocks and challenges. In A. Soares, editor, *Geostatistics Tróia '92*, volume 1, pages 213–224. Kluwer.
- Journel, A. G., 1983, Nonparametric estimation of spatial distribution. *Mathematical Geology*, 15(3):445–468.
- Journel, A. G., 1989, *Fundamentals of Geostatistics in Five Lessons*. Volume 8 Short Course in Geology. American Geophysical Union, Washington, D. C..
- Journel, A. G., 2002, Combining knowledge from diverse sources: An alternative to traditional data independence hypotheses. *Mathematical Geology*, 34(5):573–596, July.
- Ramoni, M., and Sebastiani, P., 2001, Robust Bayes classifiers. *Artificial Intelligence*, 125:209–226.
- Srivastava, R. M., 1994, An annealing procedure for honouring change of support statistics in conditional simulation. In R. Dimitrakopoulos, editor, *Geostatistics for the Next Century*, pages 277–290. Kluwer, Dordrecht, Holland.
- Strebelle, S., and Journel, A. G., 2000, Sequential simulation drawing structures from training images. In *6th International Geostatistics Congress*, Cape Town, South Africa, April. Geostatistical Association of Southern Africa.